Structural implications of weak Ca^{2+} block in *Drosophila* cyclic nucleotide–gated channels

Yee Ling Lam,[1] Weizhong Zeng,[1,2] Mehabaw Getahun Derebe,[1] and Youxing Jiang[1,2]

[1]Department of Physiology and [2]Howard Hughes Medical Institute, University of Texas Southwestern Medical Center, Dallas, TX 75390

Calcium permeability and the concomitant calcium block of monovalent ion current ("Ca^{2+} block") are properties of cyclic nucleotide–gated (CNG) channel fundamental to visual and olfactory signal transduction. Although most CNG channels bear a conserved glutamate residue crucial for Ca^{2+} block, the degree of block displayed by different CNG channels varies greatly. For instance, the *Drosophila melanogaster* CNG channel shows only weak Ca^{2+} block despite the presence of this glutamate. We previously constructed a series of chimeric channels in which we replaced the selectivity filter of the bacterial nonselective cation channel NaK with a set of CNG channel filter sequences and determined that the resulting NaK2CNG chimeras displayed the ion selectivity and Ca^{2+} block properties of the parent CNG channels. Here, we used the same strategy to determine the structural basis of the weak Ca^{2+} block observed in the *Drosophila* CNG channel. The selectivity filter of the *Drosophila* CNG channel is similar to that of most other CNG channels except that it has a threonine at residue 318 instead of a proline. We constructed a NaK chimera, which we called NaK2CNG-Dm, which contained the *Drosophila* selectivity filter sequence. The high resolution structure of NaK2CNG-Dm revealed a filter structure different from those of NaK and all other previously investigated NaK2CNG chimeric channels. Consistent with this structural difference, functional studies of the NaK2CNG-Dm chimeric channel demonstrated a loss of Ca^{2+} block compared with other NaK2CNG chimeras. Moreover, mutating the corresponding threonine (T318) to proline in *Drosophila* CNG channels increased Ca^{2+} block by 16 times. These results imply that a simple replacement of a threonine for a proline in *Drosophila* CNG channels has likely given rise to a distinct selectivity filter conformation that results in weak Ca^{2+} block.

INTRODUCTION

CNG channels are nonselective cation channels gated by cAMP or cGMP (Fesenko et al., 1985; Haynes and Yau, 1985; Yau and Nakatani, 1985; Nakamura and Gold, 1987; Dryer and Henderson, 1991; Kaupp and Seifert, 2002). Many members of the channel family have long been established to be a key component of phototransduction and olfactory signaling. In these signaling cascades, stimuli from the environment such as light or odorant trigger a change in the cellular cyclic nucleotide concentration. The resulting opening or closing of the CNG channels leads to a change in ion concentrations and membrane potential that propagates and amplifies downstream signaling.

In physiological conditions, CNG channels primarily conduct Na^+ and Ca^{2+}, with higher selectivity for Ca^{2+}. The preference for Ca^{2+} enables a significant amount of Ca^{2+} to permeate through CNG channels, even though the extracellular Ca^{2+} concentration is 60 times lower than that of Na^+. The influx of Ca^{2+} is important for the functions of many CNG channels, including the olfactory and plant CNG channels, in which Ca^{2+} directly binds to the next signaling protein downstream (Kaupp and Seifert, 2002; Ma, 2011; Moeder et al., 2011). The high selectivity for Ca^{2+} is associated with a slow permeation rate in CNG channels (Frings et al., 1995; Dzeja et al., 1999). In the presence of Ca^{2+}, the slow Ca^{2+} permeation rate drastically reduced the Na^+ current, resulting in an apparent Ca^{2+} block of monovalent ion current. In the visual sensory system, this phenomenon of Ca^{2+} block is thought to reduce the channel conductance, giving rise to low membrane potential noise that allows photoreceptor cells to detect light with high sensitivity (Yau and Baylor, 1989). Although Ca^{2+} block is observed in most common CNG channels, different CNG channels exhibit a wide range of Ca^{2+} sensitivity (Frings et al., 1995; Dzeja et al., 1999). The mechanism underlying the differences in Ca^{2+} block among different CNG channels is not entirely clear. It has been established that the glutamate residues in the selectivity filter sequence TIGETPPP are responsible for the Ca^{2+} block (Root and MacKinnon, 1993; Eismann et al., 1994; Gavazzo et al., 2000). Neutralizing this glutamate

Correspondence to Youxing Jiang: youxing.jiang@utsouthwestern.edu

M.G. Derebe's present address is Janssen Pharmaceuticals, Spring House, PA 19477.

Abbreviation used in this paper: DmCNGA, *Drosophila melanogaster* CNG channel.

The Rockefeller University Press $30.00
J. Gen. Physiol. Vol. 146 No. 3 255–263
www.jgp.org/cgi/doi/10.1085/jgp.201511431

to asparagine diminishes external Ca^{2+} block (Root and MacKinnon, 1993; Eismann et al., 1994; Gavazzo et al., 2000), whereas mutating it to aspartate enhances the block (Root and MacKinnon, 1993; Picco et al., 2001).

In the absence of a CNG channel structure, insight into the structural details underlying ion nonselectivity and Ca^{2+} block has been limited to K^+ channel models (Doyle et al., 1998; Zhou et al., 2001; Long et al., 2007) and more recently the prokaryotic nonselective cation channel NaK from *Bacillus cereus* (Shi et al., 2006; Alam et al., 2007). These bacterial channels have a topology very similar to CNG channel pore domain, even though they lack the cyclic nucleotide–binding domain. By using NaK as the model system, we have engineered a set of CNG-mimicking NaK chimeras, NaK2CNG, in which the NaK selectivity filter sequence was replaced with those of canonical CNG channels, and we determined their structures to high resolution (Derebe et al., 2011). In one such chimera named NaK2CNG-E, the NaK filter sequence of TVGDGNFSP was replaced with TVGETPPP to simulate the most commonly seen CNG channel pores (Fig. 1). The resulting mutant faithfully recapitulated the selectivity and Ca^{2+}-blocking property of canonical CNG channels, and the Ca^{2+}-blocking sensitivity can be similarly modulated by changing the glutamate residues in the filter to aspartate (NaK2CNG-D) or asparagine (NaK2CNG-N) (Derebe et al., 2011).

However, the glutamate residue in the selectivity filter is unlikely to be the only factor that governs the Ca^{2+} block of monovalent ion current. One intriguing example is that even though the *Drosophila melanogaster* CNG channel (DmCNGA) has the highly conserved glutamate in its filter sequence, the channel shows weak Ca^{2+} block (Baumann et al., 1994; Dzeja et al., 1999). A sequence alignment of *Drosophila* and other vertebrate species of CNG channels showed that *Drosophila* has a filter sequence of TIGETPT_{318}P, whereas most other species have a sequence of TIGETPPP (Fig. 1). In this study, we engineered a *Drosophila* CNG-mimicking NaK chimera named NaK2CNG-Dm, which contains a filter sequence of TVGETPTP. NaK2CNG-Dm adopted a filter structure very different from NaK2CNG-E, and the channel exhibited weak Ca^{2+} block similar to *Drosophila* CNG channels. To confirm that the presence of threonine in the filter is the cause of the reduced Ca^{2+} block in *Drosophila* CNG channels, we mutated threonine 318 to proline in DmCNGA and generated a gain-of-function mutant. This mutant has strong Ca^{2+} block like canonical CNG channels, which validated our prediction based on NaK2CNG-Dm structure and function.

MATERIALS AND METHODS

Protein expression and purification

NaK2CNG-Dm is generated by making a P69T mutation of NaK2CNG-E, which is in the background of NaKNΔ19 in vector pQE60. Details of the construct have been described previously (Alam and Jiang, 2009a; Derebe et al., 2011). For functional studies, both NaK2CNG-E and NaK2CNG-Dm have an extra F92A mutation, which increased the flux and facilitated channel recording (Alam and Jiang, 2009a,b). All constructs were expressed in XL1blue cells. 5 mM $BaCl_2$ was added to media to achieve optimal expression. The cells were induced 8–10 h after inoculation with the addition of 0.4 mM IPTG at 25°C for 16 h. Cells were then harvested and lysed by sonication in 100 mM KCl, 50 mM Tris, pH 8.0, DNaseI, and protease inhibitors including leupeptin, pepstatin, aprotinin, and PMSF (Sigma-Aldrich). The expressed protein was solubilized with 40 mM *n*-decyl-β-D-maltoside (DM; Anatrace) for 3 h at room temperature and purified on a Talon Co^{2+} affinity column (Takara Bio Inc.). The eluted protein was incubated overnight in 4°C with 2 U thrombin (Roche) for the removal of the histidine tag. The cleaved protein was then further purified by a Superdex 200 (10/30) size-exclusion column (GE Healthcare) equilibrated with 100 mM KCl, 20 mM Tris, pH 8.0, and 4 mM DM.

Protein crystallization, data collection, and structural determination

Protein was concentrated to ~15 mg/ml using a centrifugal filtration device (50-kD molecular mass cutoff; Amicon Ultra; EMD

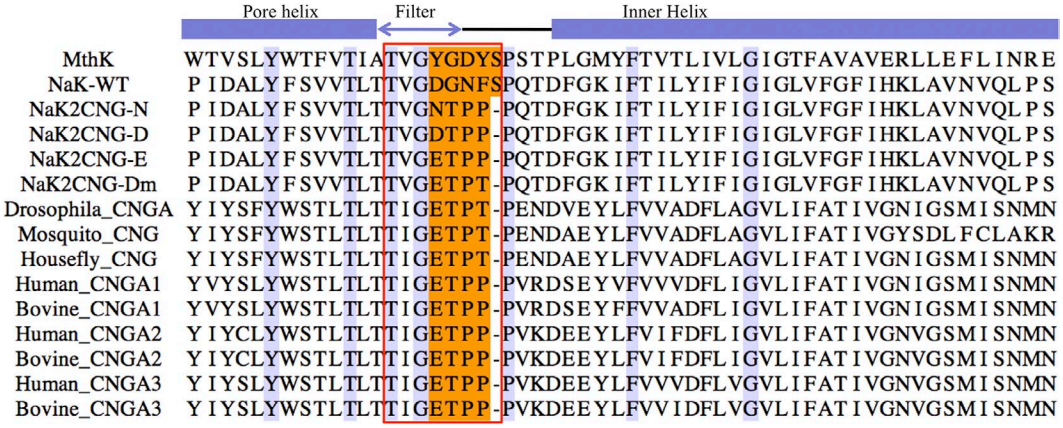

Figure 1. Partial sequence alignment of potassium channel MthK, NaK, NaK2CNG chimeras, CNG channels of *Drosophila*, mosquito, housefly, human, and bovine. Residues conserved in all channels are shaded in violet. Boxed in red are the selectivity filter sequences. Residues shaded in orange in the NaK sequence are replaced, respectively, by the shaded residues in CNG channels.

Millipore) and crystallized at 20°C using the sitting-drop vapor diffusion method. Equal volumes of concentrated protein and well solution containing 65–72.5% (±)-2-methyl-2,4-pentanediol, 100 mM buffer, pH 8–9.5 (Tris or HCl for pH 8.0–8.5 and glycine for pH 9.0–9.5), and 100 mM KCl. All crystals were frozen in liquid nitrogen with the crystallization solution serving as the cryoprotectant. Crystals were of space group I4 with unit cell dimensions around a = b = 68 Å and c = 89 Å, and they contained two molecules per asymmetric unit. Multiple x-ray diffraction data were collected at various synchrotron facilities, and the data used for final refinement were collected at the Advanced Photon Source beamline 23ID. Data were processed and scaled in HKL2000 (HKL Research, Inc.; Otwinowski and Minor, 1997). The structures were determined by molecular replacement using the NaK2CNG-E structure as an initial search model followed by repeated cycles of model refinement using Phenix (Adams et al., 2010). All structural figures and the video were generated in PyMOl (Molecular Graphics System; Schrödinger, LLC).

Although the channel was crystallized in the presence of K^+ salt, the electron density at site 3 is too strong to be accounted for as solely K^+, indicating a partial occupancy of a heavy atom. Similar strong density was also observed in NaK channel previously (Alam and Jiang, 2009a). We suspected that the heavy atom contaminant is Ba^{2+}, which is known to bind NaK and K^+ channel pores, and was added to cell culture during protein expression. Nevertheless, in this study we still model the site 3 density as K^+ for simplicity.

It is also worth noting that most CNG channels contain an Ile residue in the filter instead of a Val as seen in NaK2CNG chimeras. In a previous study, we generated a NaK2CNG chimera bearing an Ile in the filter and confirmed that Ile-to-Val interchange does not introduce any structural alterations in protein packing around the selectivity filter (Derebe et al., 2011).

Liposome reconstitution and electrophysiology

Lipid vesicles composed of a 3:1 (wt/wt) ratio of 1-palmitoyl-2-oleoyl-phosphatidylethanolamine and 1-palmitoyl-2-oleoyl-phosphatidylglycerol (Avanti Polar Lipids, Inc.) was air dried in argon gas and a SpeedVac (Thermo Fisher Scientific) for 1.5–2 h. Dried lipid was resuspended in 100 mM KCl and 20 mM Tris, pH 8.0, sonicated in water bath, and incubated with 10 mM DM. Purified proteins were then reconstituted into the lipid mixture in a protein/lipid ratio of 0.1–1 µg/mg. Reconstituted liposomes were dialyzed in 100 mM KCl and 20 mM Tris, pH 8.0, for 72 h, with buffer change every 24 h. Single-channel currents were recorded on proteoliposomes at a 1:1,000–10,000 (wt/wt) protein/lipid ratio using giant liposome patch clamp. Giant liposomes were formed by drying proteoliposomes on a clean coverslip overnight at 4°C followed by rehydration at room temperature. The standard bath solution contained 150 mM KCl, 0.5 mM EGTA, and 10 mM HEPES-KOH, pH 7.4. The patch pipettes were pulled from borosilicate glass (Harvard Apparatus) with a resistance of 8–12 MΩ and filled with 150 mM NaCl, 0.5 mM EGTA, and 10 mM HEPES-NaOH, pH 7.4. In the study of extracellular Ca^{2+} block, various concentrations of Ca^{2+} were added to the bath solution. The free Ca^{2+} concentration in the range of 0–100 µM was controlled by mixing 5 mM EGTA with an appropriate amount of $CaCl_2$, calculated using the software MAXCHELATOR (Patton et al., 2004; Bers et al., 2010). The giga-seal (>10 GΩ) was formed by gentle suction when the patch pipette was attached to the giant liposome. To get a single layer of membrane patch, the pipette was pulled away from the giant liposome, and the patch pipette tip was exposed to air for 1–2 s. Data were acquired using an amplifier (AxoPatch 200B; Molecular Devices) with the low-pass analogue filter set to 1 kHz. The current signal was sampled at a rate of 20 kHz using a digitizer (Digidata 1322A; Molecular Devices) and further analyzed with pClamp 9 software (Molecular Devices). Because of the two possible orientations of reconstituted NaK2CNG mutants in the liposomes, 30 µM tetrapentyl ammonium, an intracellular pore blocker for NaK CNG channels, was also added in the bath solution to ensure that the channel in the recording had its extracellular side facing the bath solution. No cyclic nucleotide was present in any of the patches because NaK2CNG-Dm does not have a cyclic nucleotide–binding domain, and its gating is not sensitive to any cyclic nucleotide.

TABLE 1
Data collection and refinement statistics

Statistic	NaK2CNG-Dm
Data Collection	
Space group	I_4
Cell Dimensions a = b, c (Å)	67.907, 89.799
Wavelength (Å)	1.0000
Resolution (Å)	50 - 1.90
R_{sym} (%)	8.6 (66.8)
I/σI	19.0 (0.97)
No. of reflections- total (unique)	283595 (15224)
Completeness (%)	95
Refinement	
Redundancy	6.5 (2.2)
Resolution (Å)	1.90
R_{work}/R_{free}	0.2038/0.2361
No. of atoms	
Protein	1448
Ion	7
Water	102
Rmsd	
Bond angles (°)	0.966
Bond lengths (Å)	0.005

Values in parenthesis are for the highest resolution shell. 5% of the data were used in the R_{free} calculation. Rmsd, root-mean-square deviation.

Functional expression in HEK 293T cells

Drosophila and bovine CNG channels were individually cloned into pEGFP-C1 vector. T318P mutation in *Drosophila* and P366T mutations in bovine CNG channels were subsequently generated using Pfu Turbo Polymerase (Agilent Technologies) and primers containing the mutations. HEK 293T cells were used to express *Drosophila* or bovine CNG-GFP fusion protein and measure CNG channels current. Recordings were done 24–48 h after transient transfection of plasmids using lipofectamine 2000 (Invitrogen). For outside-out and whole-cell configuration, the pipette contained 140 mM KCl, 5 mM EGTA, 10 mM HEPES, pH 7.4, and 1 mM cGMP. The bath solution contained 140 mM NaCl, 4 mM KCl, 1 mM EGTA, and 10 mM HEPES, pH 7.4. For the inside-out and cell-attached configuration, the pipette contained 140 mM NaCl, 4 mM KCl, 1 mM EGTA, and 10 mM HEPES, pH 7.4, whereas the bath solution contained 140 mM KCl, 5 mM EGTA, and 10 mM HEPES, pH 7.4. In the study of extracellular Ca^{2+} block, various concentrations of Ca^{2+} were added to the bath solution in the same manner as in the giant liposome patch-clamp experiment described above. Data were also acquired and analyzed using the same device and method as in the giant liposome patch-clamp experiment described above.

Data deposition

The atomic coordinates and structural factors of NaK2CNG-Dm have been deposited in the Protein Data Bank (accession no. 4ZBM).

Online supplemental material

Video 1 shows the overall structure of NaK2CNG and the morphing from the selectivity filter structure of NaK2CNG-E to that of

NaK2CNG-Dm. Fig. S1 shows that the single-channel recordings from the cell-attached patch data presented in Fig. 5 are cGMP sensitive and are indeed from CNG channels. The online supplemental material is available at http://www.jgp.org/cgi/content/full/jgp.201511431/DC1.

RESULTS

NaK2CNG-Dm has a unique filter structure

To model the *Drosophila* CNG channel pore, we replaced the selectivity filter of NaK with that of *Drosophila* CNG channel and named the construct NaK2CNG-Dm. NaK2CNG-Dm has a filter sequence of $_{63}$TVGETPT$_{69}$, which, in essence, is a P69T mutation of NaK2CNG-E. The structure of NaK2CNG-Dm in complex with K^+ was determined to 1.9 Å (Table 1). Although it maintains the same overall structure as NaK (Fig. 2 A), the selectivity filter of NaK2CNG-Dm adopts a novel conformation distinct from that of wild-type NaK, our previous NaK2CNG chimeras, and potassium channel NaK2K (Fig. 2, B and C). The first two filter residues (Thr63 and Val64) of NaK2CNG-Dm form two ion-binding sites (sites 3 and 4) at the internal half of the filter, which are virtually identical to those of other channels. However, the NaK2CNG-Dm filter has a unique external half, where the $_{65}$GET filter residues adopt a novel main-chain conformation and generate a deep funnel-shaped entrance filled with layers of ordered water molecules and hydrated K^+ ions (Fig. 2 B). This entrance is much deeper and wider than that of the other NaK2CNG mutants such as NaK2CNG-E, to which the detailed structural comparison is made below.

Although NaK2CNG-E and NaK2CNG-Dm differ only at residue 69, the major structural divergence occurs at the $_{65}$GET region, several residues before Thr69, where both channels have identical sequence. As shown in the structural superimposition, the $_{65}$GET peptides of the two channel filters adopt a nearly inverted main-chain

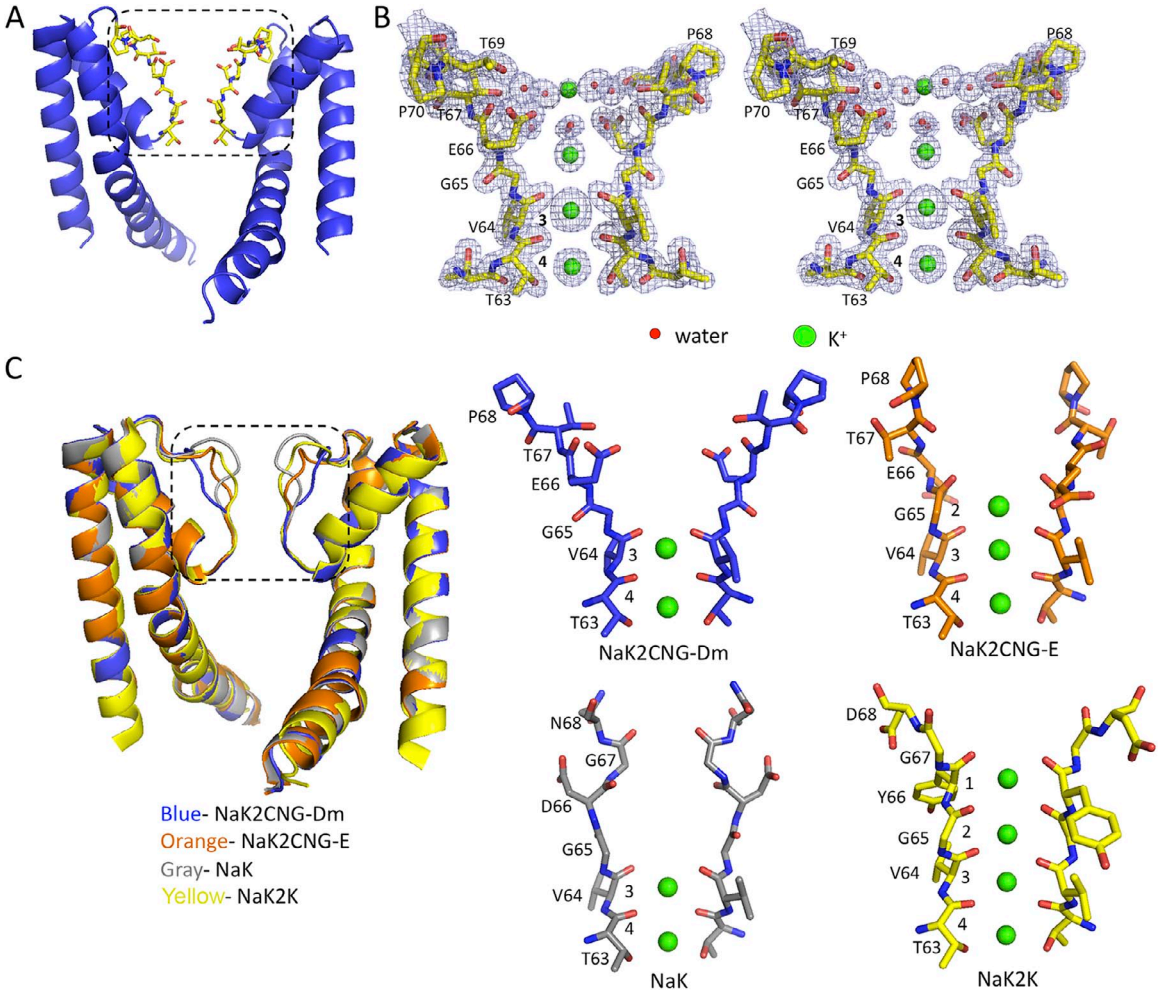

Figure 2. Structure of NaK2CNG-Dm. (A) Overall structure of NaK2CNG-Dm, with the front and back subunit removed for clarity. (B) A stereo view of the selectivity filter region boxed in A. $2F_o$-Fc (2σ) electron density map is shown in mesh. (C; left), Superimposition of NaK2CNG-Dm (blue), NaK2CNG-E (orange), wild-type NaK (gray), and potassium channel NaK2K (yellow) shows that the four channels differ mainly at the filter region (boxed). (Right) The selectivity filters of NaK2CNG-Dm, NaK2CNG-E, NaK, and NaK2K adopt different conformations at the external half and consequently have varying numbers of ion-binding sites.

conformation, and the structural change involves an almost 180° rotation of the GET peptide, with the pivot point at the Cα of Gly65 (Fig. 3 A). Consequently, there are four major structural differences between the filters of the two channels. First, in NaK2CNG-E, the backbone carbonyl oxygen atom of Gly65 points toward the center of the ion permeation pathway and forms the top layer of the ion ligand at site 2, yet in NaK2CNG-Dm, it flips away from the center, abolishing the ion-binding site (Fig. 2 C). Second, the side chain of Glu66 points downward toward the pore helix in NaK2CNG-E but points outward to the external solution and lies on the surface of the external funnel entrance in NaK2CNG-Dm. Third, the reorientation of Glu66 is associated with the formation of a completely new set of packing interactions (Fig. 3, B and C). In NaK2CNG-E, the Glu66 carboxylate side chain forms hydrogen bonds with Thr60 of the neighboring subunit, and its backbone carbonyl forms a hydrogen bond with Tyr55 of the same subunit. In NaK2CNG-Dm, the carboxylate group of Glu66 forms a new hydrogen-bonding network with Thr67 and Tyr55 of the neighboring subunit as well as Thr69 of the same subunit. Fourth, to accommodate the dramatic main-chain conformational change, the peptide bond between Thr67 and Pro68 changes from trans configuration in NaK2CNG-E to cis configuration in NaK2CNG-Dm. The significance of all these structural differences can be implied from the difference in ion permeation property between the two channels as described below.

Ion permeation and Ca^{2+} block in NaK2CNG-Dm

Giant liposome patch clamp was used to assay the ion permeation and Ca^{2+}-blocking properties of the NaK2CNG-Dm channel. Similar to NaK2CNG-E, NaK2CNG-Dm has high open probability and exhibits some subconductance states (Fig. 4 A). Under bi-ionic condition with 150 mM KCl in bath and 150 mM NaCl in pipette, NaK2CNG-Dm has a single-channel conductance of ∼56 pS for inward K^+ current at −100 mV, much smaller than that of NaK2CNG-E (∼100 pS) measured previously under the same condition (Derebe et al., 2011). Interestingly, NaK2CNG-Dm is weakly selective for K^+ with a reversal potential of 25 mV, corresponding to P_K/P_{Na} of ∼2.7 (Fig. 4 B). This is in contrast to NaK2CNG-E, which was reported previously to be nonselective (Derebe et al., 2011). The Ca^{2+} block of NaK2CNG-Dm was measured

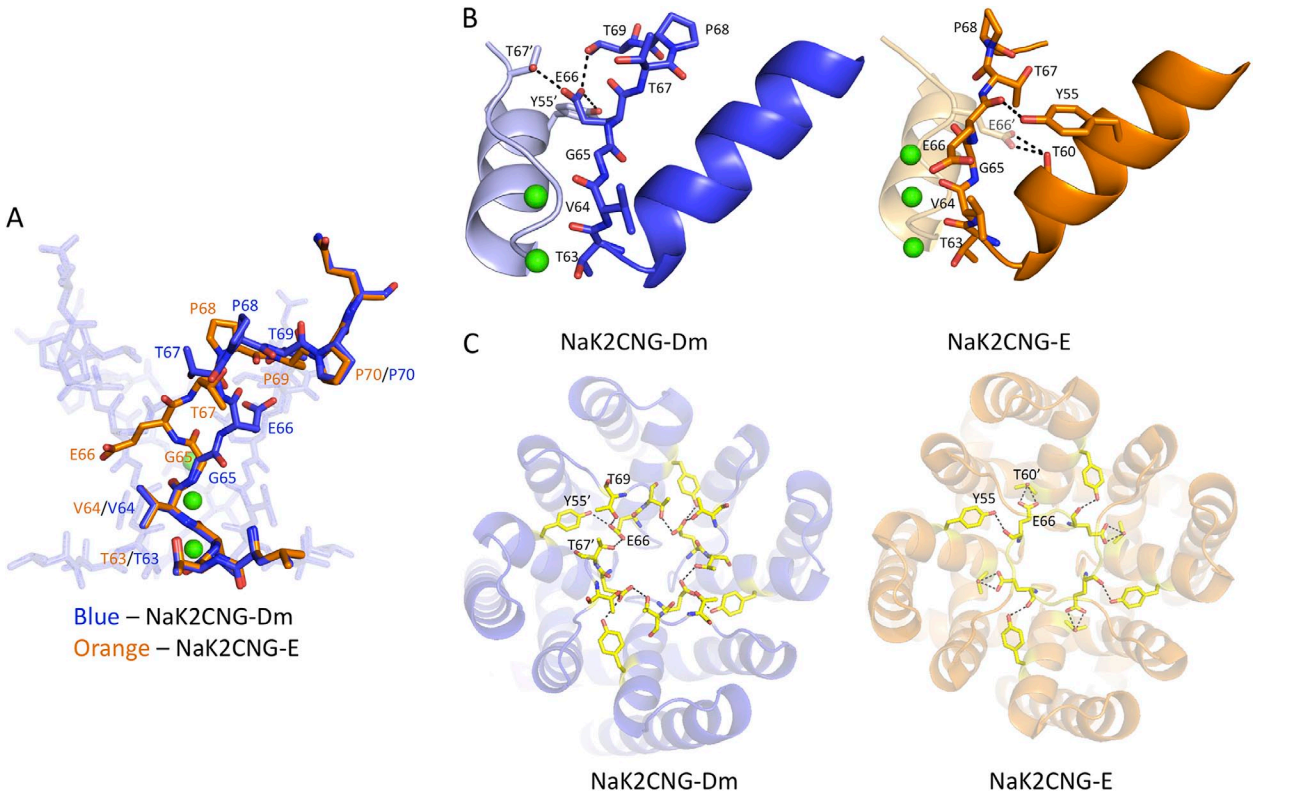

Figure 3. Structural comparison of NaK2CNG-Dm and NaK2CNG-E. (A) Superimposition of NaK2CNG-Dm (blue) and NaK2CNG-E (orange) at the selectivity filter region, showing the divergence of the main-chain backbones at the $_{65}$GET region. The superimposition is highlighted for the front subunit, and the other subunits of NaK2CNG-Dm are shaded in light blue in the background. (B) Comparison of the selectivity filter of one subunit from NaK2CNG-Dm and NaK2CNG-E. Dashed lines indicate the hydrogen bonds between Glu66 and surrounding residues. Residues from a neighboring subunit are marked with single quotation marks. (C) A comparison of the hydrogen-bonding network of NaK2CNG-Dm and NaK2CNG-E, viewed from the external side of the channel tetramers. Residues involved in the hydrogen bonds are displayed as yellow sticks.

with various concentrations of Ca^{2+} added to the external side of the channel (bath solution). As shown in Fig. 4 (C and D), Ca^{2+} only weakly blocked the monovalent ion current in NaK2CNG-Dm with a K_i of ~4 ± 0.6 mM, which is in stark contrast with the K_i of 59 ± 10 µM in NaK2CNG-E.

T318P mutation strengthens Ca^{2+} block in *Drosophila* CNG channels

To test if the presence of threonine instead of proline is responsible for the weak Ca^{2+} block in *Drosophila* CNG channel as in the NaK2CNG model system, we mutated threonine 318 (equivalent to T69 in NaK2CNG-Dm) in DmCNGA to proline (T318P) so that its filter sequence became TIGETPP$_{318}$P. The mutant channel was heterologously expressed in HEK293T cells. Single-channel recordings in cell-attached configuration demonstrated that the mutant channel has kinetic properties similar to the wild-type channel, but the single-channel conductance increased from 17 pS in wild type to 21 pS in T318P mutant at −100 mV (Fig. 5 A). The dose–response to cGMP-regulated gating, on the other hand, was not affected by the mutation, as confirmed by the $[cGMP]_i$-dependent inward currents in inside-out patches (Fig. 5 B). However, based on the whole-cell recording results, the single mutation resulted in a significant enhancement in external Ca^{2+} block, as demonstrated in the I-V curves of wild-type DmCNGA and T318P mutant in the presence of varying external $[Ca^{2+}]$ (Fig. 5 C). The plot of the unblocked inward current at −80 mV as a function of external $[Ca^{2+}]$ yields a K_i of 229 ± 25 µM for wild-type DmCNGA and 13.7 ± 2.2 µM for the T318P mutant (Fig. 5 D). The 16-fold increase in Ca^{2+}-blocking affinity is reminiscent of the difference in Ca^{2+}-blocking sensitivity between NaK2CNG-E and NaK2CNG-Dm, implying that the altered filter structure observed in NaK2CNG-Dm is probably the reason for the weak Ca^{2+} block in *Drosophila* CNGA.

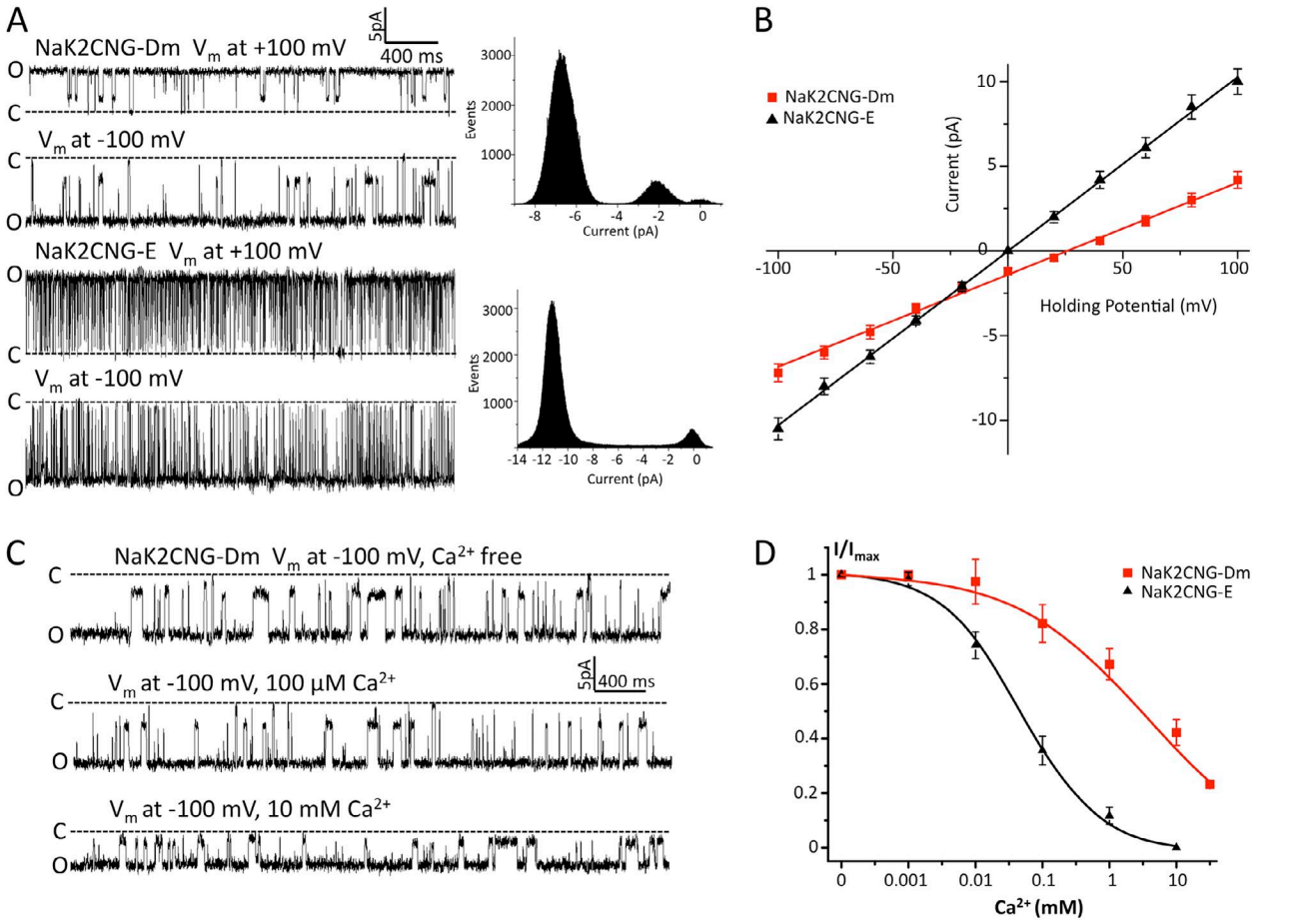

Figure 4. Ion conduction and Ca^{2+} block of NaK2CNG-Dm. (A; left) Sample traces of single-channel recordings of NaK2CNG-Dm and NaK2CNG-E at ±100 mV. (Right) Histogram of single-channel current at −100 mV. (B) Ion selectivity and conductance of NaK2CNG-Dm and NaK2CNG-E are compared in I-V plot. Error bars are the mean ± SEM of five independent measurements. (C) Sample traces of single-channel recordings at −100 mV at different external (bath) Ca^{2+} concentrations. (D) Fraction of unblocked current (I/I_{max}) at −100 mV as a function of Ca^{2+} concentration. Data are fitted into a Hill equation, with K_i of 4 ± 0.6 mM and a Hill coefficient n of 0.52 for NaK2CNG-Dm and K_i of 59 ± 10 µM and n of 0.98 for NaK2CNG-E. Error bars are mean ± SEM from five measurements.

P366T mutation has weak effect on Ca^{2+} block in bovine CNGA1

Because threonine 318 in *Drosophila* was found to be the key in gauging Ca^{2+} block, we asked whether the equivalent residue in mammalian CNG channels is important for the block. This was tested on bovine CNGA1 channel by replacing the equivalent proline (P366) with threonine, resulting in a selectivity filter sequence of TIGETPTP. The P366T mutation in bovine CNGA1 has no obvious effect on single-channel conductance and kinetics or cGMP-regulated gating (Fig. 6, A and B). However, contrary to our prediction based on the NaK2CNG mutants as well as the mutation on *Drosophila* CNGA, the Pro-to-Thr replacement in bovine CNGA1 has almost no effect on Ca^{2+} block. Outside-out patch recordings show that mutation only results in a subtle decrease of Ca^{2+} affinity (K_i = 3.5 ± 0.5 µM for wild type and K_i = 6.0 ± 0.7 µM for P366T; Fig. 6, C and D), suggesting that the equivalent Thr/Pro swap in CNGA1 does not compromise the structure integrity of the filter, and the channel thereby retains its strong Ca^{2+} block.

DISCUSSION

In this study, we aimed to understand the origin of the weak Ca^{2+} block found in *Drosophila* CNG channels (Root and MacKinnon, 1993; Eismann et al., 1994; Gavazzo et al., 2000). Like most other CNG channels, *Drosophila* CNG channel has the highly conserved glutamate residue known to be important for Ca^{2+} binding but has one of the weakest Ca^{2+} block compared with other well-studied CNG channels such as the mammalian CNGA1 and CNGA2 (Baumann et al., 1994; Dzeja et al., 1999). Such variation implies the presence of other residue(s) that can modulate Ca^{2+} block and permeability in CNG channels.

Here, we provide structural insights into the weak Ca^{2+} block in *Drosophila* CNG channels by determining the structure of *Drosophila* CNG pore-mimicking NaK mutant, NaK2CNG-Dm. Compared with our previously established CNG-mimicking NaK model (i.e., NaK2CNG-E), NaK2CNG-Dm adopts a very different selectivity filter structure, resulting in a much weaker Ca^{2+} binding and a reduction in single-channel conductance. The significantly changed filter conformation

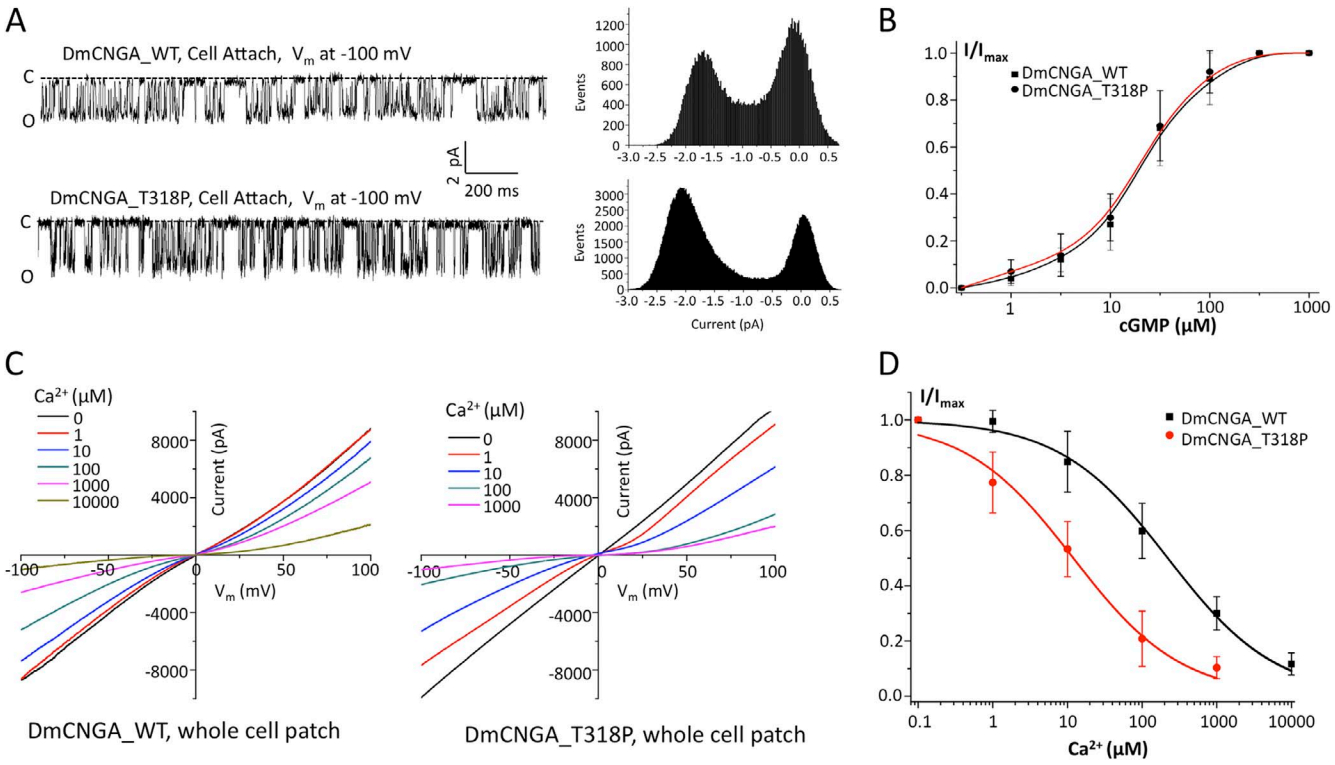

Figure 5. Functional comparison of DmCNGA and T318P mutant. (A; left) Sample traces of single-channel recordings of DmCNGA and T318P mutant at −100 mV in cell-attached configuration. (Right) Histogram of single-channel current at −100 mV. (B) Normalized macroscopic currents of wild-type DmCNGA and T318P mutant as a function of $[cGMP]_i$ measured in inside-out patches at −100 mV. Data are fitted to the Hill equation. The $K_{1/2}$ and n of DmCNGA are 16.4 ± 1.8 µM and 1.3, respectively. The $K_{1/2}$ and n of T318P mutant are 15.2 ± 2.1 µM and 1.2, respectively. (C) I-V curves of DmCNGA and T318P mutant measured from whole-cell recordings at different external (bath) Ca^{2+} concentrations. (D) Fraction of unblocked current (I/I_{max}) at −100 mV as a function of external Ca^{2+} concentration. Data are fitted into a Hill equation with, K_i of 229.5 ± 25 µM and n of 0.62 for DmCNGA and K_i of 13.7 ± 2.2 µM and n of 0.59 for T318P. All error bars are mean ± SEM from five measurements.

was unexpected, considering the fact that NaK2CNG-E and NaK2CNG-Dm differ by only one residue. This residue, positioned immediately outside of the selectivity filter, is a proline in NaK2CNG-E and most CNG channels but a threonine in NaK2CNG-Dm and in a subset of CNG channels from *Drosophila* and several other insects (Fig. 1). We reason that the weak Ca^{2+} block observed in DmCNGA originates from a filter structure different from canonical CNG channels because of the presence of the threonine (T318) instead of proline. By having a threonine, the selectivity filter sequence of *Drosophila* ends with "PTP" rather than three consecutive prolines as in canonical CNG channel filter sequence "TIGETPPP." The PTP sequence probably enjoys a larger degree of flexibility than PPP, as the unique side chain of proline tends to restrict backbone conformation. We speculate that the middle threonine of the *Drosophila* sequence is pivotal to provide flexibility sufficient for a segment of the backbone to adopt a flipped conformation, which would be impossible if it were a proline.

The importance of the threonine was tested by replacing Thr318 with proline in DmCNGA, and the resulting mutant channel showed both an increase in single-channel conductance and a >16-fold increase in Ca^{2+} affinity. This striking gain-of-function mutation has brought the Ca^{2+} block of DmCNGA on par with that of the mammalian CNG channels such as CNGA1, implying that DmCNGA T318P has likely adopted a filter structure similar to NaK2CNG-E. This threonine that is critical for the filter structure does not locate inside the filter for direct ion binding, nor does it involve any change of electrical charge. Without the structural guidance from those CNG-mimicking NaK mutants, it is inconceivable to predict that such mutation in DmCNGA can have a profound effect on Ca^{2+} binding.

Interestingly, the reversed proline (P366) to threonine mutation at the equivalent position of bovine CNGA1 affects neither the Ca^{2+} block nor the single-channel conductance of the channel, suggesting that the filter structure of the mutant has likely remained the same as wild type. As Ca^{2+} block of CNG channels appears to be governed by multiple factors and residues, this result is not unexpected. The structural differences between NaK2CNG-E and NaK2CNG-Dm involve dramatic alteration of the main-chain conformation as well as rearrangement of packing interactions at the filter regions. Therefore, the surrounding residues are expected to play important roles in stabilizing the filter. We speculate that there are additional structural elements in bovine CNG channels that stabilize the filter and prevent it from

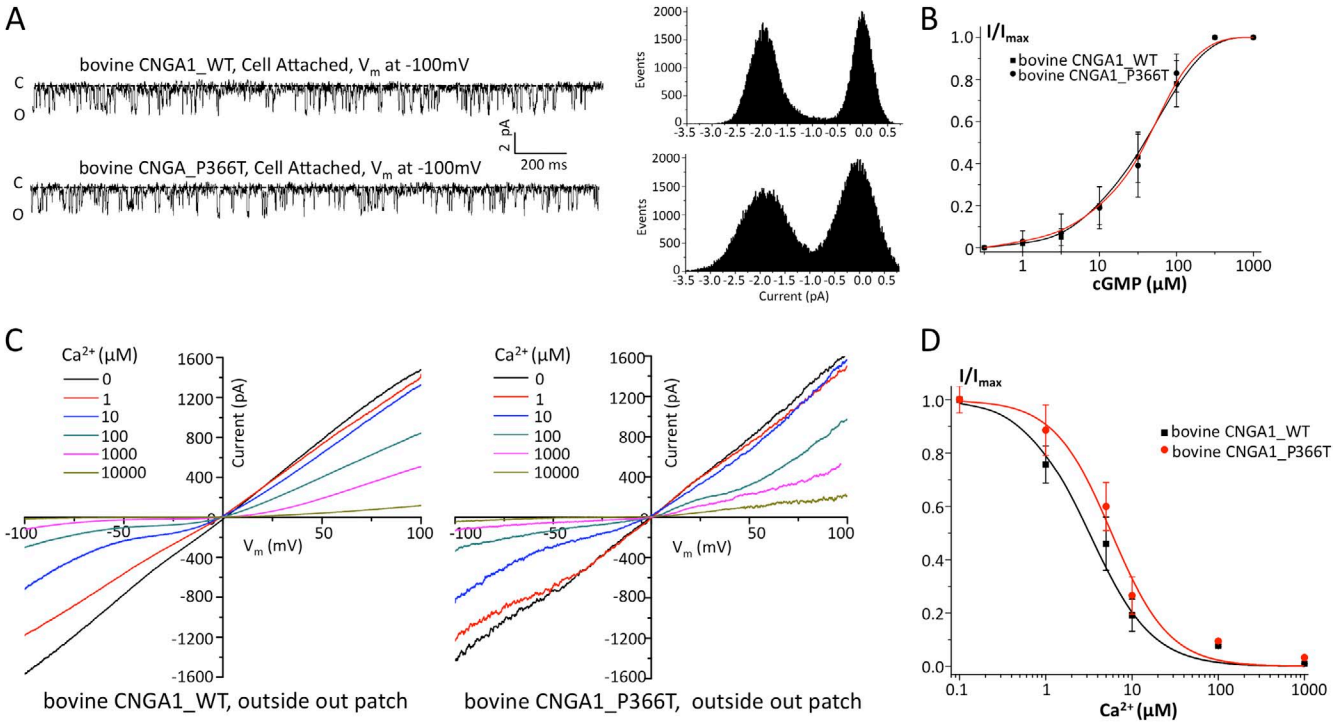

Figure 6. Functional comparison of bovine CNGA1 and P366T mutant. (A; left) Sample traces of single-channel recordings of bovine CNGA1 and P366T at −100 mV in cell-attached configuration. (Right) Histogram of single-channel current at −100 mV. (B) Normalized macroscopic currents of wild-type bovine CNGA1 and P366T mutant as a function of $[cGMP]_i$ measured in inside-out patches at −100 mV. Data are fitted to the Hill equation. The $K_{1/2}$ and n of bovine CNGA1 are 39.5 ± 3.6 μM and 1.2, respectively. The $K_{1/2}$ and n of P366T are 41.2 ± 4.7 μM and 1.3, respectively. (C) I-V curves of bovine CNGA1 and P366T mutant measured from outside-out patches at different external (bath) Ca^{2+} concentrations. (D) Fraction of unblocked current (I/I_{max}) at −100 mV as a function of Ca^{2+} concentration. Data are fitted into a Hill equation, with K_i of 3.5 ± 0.5 μM and n of 1.03 for bovine CNGA1 and K_i of 6.0 ± 0.7 μM and n of 1.36 for P366T. All error bars are mean ± SEM from five measurements.

undergoing structural rearrangement upon mutation. Because most selectivity filters of CNG channels are highly similar in sequence, future studies would focus on residues that are outside of the selectivity filter but interact with the filter residues. These residues are likely the determinants of the conformational flexibility of the filter and are thus the best candidates to provide leads that will allow us to further dissect the mechanism of Ca^{2+} block in CNG channels.

Results shown in this paper are derived from work performed at Argonne National Laboratory, Structural Biology Center (19ID) and GM/CA (23ID) at the Advanced Photon Source, and from work performed at the Berkeley Center for Structural Biology at the Advanced Light Source. Argonne is operated by UChicago Argonne, LLC, for the US Department of Energy, Office of Biological and Environmental Research under contract number DE-AC02-06CH11357. The Berkeley Center for Structural Biology is supported in part by the National Institutes of Health (NIH), National Institute of General Medical Sciences, and the Howard Hughes Medical Institute. The Advanced Light Source is supported by the Director, Office of Science, Office of Basic Energy Sciences, of the US Department of Energy under contract number DE-AC02-05CH11231. This work was supported in part by the Howard Hughes Medical Institute and by grants from the NIH (GM079179 to Y. Jiang) and the Welch Foundation (I-1578 to Y. Jiang).

The authors declare no competing financial interests.

Sharona E. Gordon served as editor.

Submitted: 1 May 2015
Accepted: 21 July 2015

REFERENCES

Adams, P.D., P.V. Afonine, G. Bunkóczi, V.B. Chen, I.W. Davis, N. Echols, J.J. Headd, L.W. Hung, G.J. Kapral, R.W. Grosse-Kunstleve, et al. 2010. PHENIX: a comprehensive Python-based system for macromolecular structure solution. *Acta Crystallogr. D Biol. Crystallogr.* 66:213–221.

Alam, A., and Y. Jiang. 2009a. High-resolution structure of the open NaK channel. *Nat. Struct. Mol. Biol.* 16:30–34. http://dx.doi.org/10.1038/nsmb.1531

Alam, A., and Y. Jiang. 2009b. Structural analysis of ion selectivity in the NaK channel. *Nat. Struct. Mol. Biol.* 16:35–41. http://dx.doi.org/10.1038/nsmb.1537

Alam, A., N. Shi, and Y. Jiang. 2007. Structural insight into Ca^{2+} specificity in tetrameric cation channels. *Proc. Natl. Acad. Sci. USA.* 104:15334–15339. http://dx.doi.org/10.1073/pnas.0707324104

Baumann, A., S. Frings, M. Godde, R. Seifert, and U.B. Kaupp. 1994. Primary structure and functional expression of a Drosophila cyclic nucleotide-gated channel present in eyes and antennae. *EMBO J.* 13:5040–5050.

Bers, D.M., C.W. Patton, and R. Nuccitelli. 2010. A practical guide to the preparation of Ca^{2+} buffers. *Methods Cell Biol.* 99:1–26. http://dx.doi.org/10.1016/B978-0-12-374841-6.00001-3

Derebe, M.G., W. Zeng, Y. Li, A. Alam, and Y. Jiang. 2011. Structural studies of ion permeation and Ca^{2+} blockage of a bacterial channel mimicking the cyclic nucleotide-gated channel pore. *Proc. Natl. Acad. Sci. USA.* 108:592–597. http://dx.doi.org/10.1073/pnas.1013643108

Doyle, D.A., J. Morais Cabral, R.A. Pfuetzner, A. Kuo, J.M. Gulbis, S.L. Cohen, B.T. Chait, and R. MacKinnon. 1998. The structure of the potassium channel: Molecular basis of K^+ conduction and selectivity. *Science.* 280:69–77. http://dx.doi.org/10.1126/science.280.5360.69

Dryer, S.E., and D. Henderson. 1991. A cyclic GMP-activated channel in dissociated cells of the chick pineal gland. *Nature.* 353:756–758. http://dx.doi.org/10.1038/353756a0

Dzeja, C., V. Hagen, U.B. Kaupp, and S. Frings. 1999. Ca^{2+} permeation in cyclic nucleotide-gated channels. *EMBO J.* 18:131–144. http://dx.doi.org/10.1093/emboj/18.1.131

Eismann, E., F. Müller, S.H. Heinemann, and U.B. Kaupp. 1994. A single negative charge within the pore region of a cGMP-gated channel controls rectification, Ca^{2+} blockage, and ionic selectivity. *Proc. Natl. Acad. Sci. USA.* 91:1109–1113. http://dx.doi.org/10.1073/pnas.91.3.1109

Fesenko, E.E., S.S. Kolesnikov, and A.L. Lyubarsky. 1985. Induction by cyclic GMP of cationic conductance in plasma membrane of retinal rod outer segment. *Nature.* 313:310–313. http://dx.doi.org/10.1038/313310a0

Frings, S., R. Seifert, M. Godde, and U.B. Kaupp. 1995. Profoundly different calcium permeation and blockage determine the specific function of distinct cyclic nucleotide-gated channels. *Neuron.* 15:169–179. http://dx.doi.org/10.1016/0896-6273(95)90074-8

Gavazzo, P., C. Picco, E. Eismann, U.B. Kaupp, and A. Menini. 2000. A point mutation in the pore region alters gating, Ca^{2+} blockage, and permeation of olfactory cyclic nucleotide-gated channels. *J. Gen. Physiol.* 116:311–326. http://dx.doi.org/10.1085/jgp.116.3.311

Haynes, L., and K.W. Yau. 1985. Cyclic GMP-sensitive conductance in outer segment membrane of catfish cones. *Nature.* 317:61–64. http://dx.doi.org/10.1038/317061a0

Kaupp, U.B., and R. Seifert. 2002. Cyclic nucleotide-gated ion channels. *Physiol. Rev.* 82:769–824. http://dx.doi.org/10.1152/physrev.00008.2002

Long, S.B., X. Tao, E.B. Campbell, and R. MacKinnon. 2007. Atomic structure of a voltage-dependent K^+ channel in a lipid membrane-like environment. *Nature.* 450:376–382. http://dx.doi.org/10.1038/nature06265

Ma, W. 2011. Roles of Ca^{2+} and cyclic nucleotide gated channel in plant innate immunity. *Plant Sci.* 181:342–346.

Moeder, W., W. Urquhart, H. Ung, and K. Yoshioka. 2011. The role of cyclic nucleotide-gated ion channels in plant immunity. *Mol. Plant.* 4:442–452.

Nakamura, T., and G.H. Gold. 1987. A cyclic nucleotide-gated conductance in olfactory receptor cilia. *Nature.* 325:442–444. http://dx.doi.org/10.1038/325442a0

Otwinowski, Z., and W. Minor. 1997. Processing of X-ray diffraction data collected in oscillation mode. *Methods Enzymol.* 276:307–326. http://dx.doi.org/10.1016/S0076-6879(97)76066-X

Patton, C., S. Thompson, and D. Epel. 2004. Some precautions in using chelators to buffer metals in biological solutions. *Cell Calcium.* 35:427–431. http://dx.doi.org/10.1016/j.ceca.2003.10.006

Picco, C., P. Gavazzo, and A. Menini. 2001. Co-expression of wild-type and mutant olfactory cyclic nucleotide-gated channels: restoration of the native sensitivity to Ca^{2+} and Mg^{2+} blockage. *Neuroreport.* 12:2363–2367. http://dx.doi.org/10.1097/00001756-200108080-00016

Root, M.J., and R. MacKinnon. 1993. Identification of an external divalent cation-binding site in the pore of a cGMP-activated channel. *Neuron.* 11:459–466. http://dx.doi.org/10.1016/0896-6273(93)90150-P

Shi, N., S. Ye, A. Alam, L. Chen, and Y. Jiang. 2006. Atomic structure of a Na^+- and K^+-conducting channel. *Nature.* 440:570–574. http://dx.doi.org/10.1038/nature04508

Yau, K.W., and D.A. Baylor. 1989. Cyclic GMP-activated conductance of retinal photoreceptor cells. *Annu. Rev. Neurosci.* 12:289–327. http://dx.doi.org/10.1146/annurev.ne.12.030189.001445

Yau, K.W., and K. Nakatani. 1985. Light-suppressible, cyclic GMP-sensitive conductance in the plasma membrane of a truncated rod outer segment. *Nature.* 317:252–255. http://dx.doi.org/10.1038/317252a0

Zhou, Y., J.H. Morais-Cabral, A. Kaufman, and R. MacKinnon. 2001. Chemistry of ion coordination and hydration revealed by a K^+ channel-Fab complex at 2.0 Å resolution. *Nature.* 414:43–48. http://dx.doi.org/10.1038/35102009